Astron. Astrophys. 351, 582–596 (1999)

ASTRONOMY AND ASTROPHYSICS

Amplitudes of stochastically excited oscillations in main-sequence stars

G. Houdek[1,2], **N.J. Balmforth**[3], **J. Christensen-Dalsgaard**[4], **and D.O. Gough**[1,5]

[1] Institute of Astronomy, University of Cambridge, Cambridge CB3 0HA, UK
[2] Institut für Astronomie, Universität Wien, 1180 Wien, Austria (hg@ast.cam.ac.uk)
[3] Instituto di Cosmogeofisica, Corso Fiume 4, Torino 10133, Italy (njb@hank.ucsd.edu)
[4] Teoretisk Astrofysik Center, Danmarks Grundforskningsfond, and Institut for Fysik og Astronomi, Aarhus Universitet, 8000 Aarhus C, Denmark (jcd@obs.aau.dk)
[5] Department of Applied Mathematics and Theoretical Physics, University of Cambridge, Cambridge CB3 9EW, UK (douglas@ast.cam.ac.uk)

Received 10 May 1999 / Accepted 7 September 1999

Abstract. We present estimates of the amplitudes of intrinsically stable stochastically excited radial oscillations in stars near the main sequence. The amplitudes are determined by the balance between acoustical energy generation by turbulent convection (the Lighthill mechanism) and linear damping. Convection is treated with a time-dependent, nonlocal, mixing-length model, which includes both convective heat flux and turbulent pressure in both the equilibrium model and the pulsations. Velocity and luminosity amplitudes are computed for stars with masses between $0.9\,M_\odot$ and $2.0\,M_\odot$ in the vicinity of the main sequence, for various metallicities and convection parameters. As in previous studies, the amplitudes are found to increase with stellar mass, and therefore with luminosity. Amongst those stars that are pulsationally stable, the largest amplitudes are predicted for a $1.6\,M_\odot$ model of spectral type F2; the values are approximately 15 times larger than those measured in the Sun.

Key words: convection – turbulence – stars: oscillations

1. Introduction

The stability of solar-like p modes depends mainly on the interaction of the oscillations with radiation and convection in the outer envelope. The most plausible explanations for the occurrence of such oscillations are either intrinsic thermal overstability or stochastic excitation of stable modes by turbulent convection. Whatever the mechanism, the energy flow from radiation and convection into and out of the p modes takes place very near the surface (e.g. Goode et al. 1992). Sun-like stars possess surface convection zones, and it is in these zones, where the energy is transported principally by the turbulence, that most of the driving takes place. Mode stability is governed not only by the perturbations in the radiative fluxes (via the κ-mechanism) but also by the perturbations in the turbulent fluxes (heat and momentum). The study of mode stability therefore demands a theory for convection that includes the interaction of the turbulent velocity field with the pulsation.

Thermal overstability of pulsations arises from an exchange of energy between the oscillatory motion of the stellar matter, the turbulence and the radiation field. Such overstability has been suggested as a possible mechanism for the excitation of solar oscillations by Ulrich (1970a) and Antia et al. (1988). If solar p modes were indeed overstable, some nonlinear mechanism must limit their amplitudes to the values that are observed. Nonlinear coupling to other, stable modes was considered by Kumar & Goldreich (1989), who estimated that the energy drain through three-mode coupling would occur at a rate too low to extract the energy gained from the overstability at the appropriate amplitude. Similar estimates of nonlinear self limiting are also too weak. The saturation of mode amplitudes at the observed levels therefore remains a mystery if overstability provides the origin of solar pulsations.

The problem of identifying a saturation mechanism does not arise if the modes are intrinsically stable. Such modes can be stochastically excited by the turbulent convection. The process can be regarded as multipole acoustical radiation (e.g. Unno 1964). For solar-like stars, the acoustic noise generated by convection in the star's resonant cavity may be manifest as an ensemble of p modes over a wide band in frequency (Goldreich & Keeley 1977b). The amplitudes are determined by the balance between the excitation and damping, and are expected to be rather low. The turbulent-excitation model predicts not only the right order of magnitude for the p-mode amplitudes (Gough 1980), but it also explains the observation that millions of modes are excited simultaneously. Moreover, recent observations (Toutain & Fröhlich 1992, Goode & Strous 1996; Chaplin et al. 1998) also support a stochastic origin. This second explanation seems therefore to be the more likely, and is the one that we shall adopt here.

To date, Christensen-Dalsgaard & Frandsen (1983b) have made the only predictions of amplitudes of solar-like oscillations in other stars. They obtained amplitudes of modes by postulating equipartition between the energy of an oscillation

Send offprint requests to: G. Houdek

mode and the kinetic energy in one convective eddy having the same turnover time as the period of the oscillation. This simple formula for excitation was proposed by Goldreich & Keeley (1977b), who used it to estimate amplitudes for the solar case, assuming damping rates determined solely by a scalar turbulent viscosity (Goldreich & Keeley 1977a). In the calculations of Christensen-Dalsgaard & Frandsen (1983b), however, radial eigenfunctions of model envelopes were computed by solving the equations of linear nonadiabatic oscillation, although they also neglected turbulent pressure and set the Lagrangian perturbation to the convective heat flux to zero. They found velocity and luminosity amplitudes to increase with age, and with increasing mass along the main sequence.

Balmforth (1992a) improved the calculation by introducing Gough's (1976, 1977) nonlocal, time-dependent mixing-length model for convection, using the Eddington approximation to radiative transfer for both the equilibrium structure and the pulsations. He calculated damping rates for the solar case and found all modes to be stable. Here we continue Balmforth's investigation and study the oscillations of main-sequence stars, delimiting the region in the HR diagram for stars with stable modes. Preliminary results of the calculations have been presented by Houdek et al. (1995).

According to Libbrecht et al. (1986) the observed oscillation properties of low-degree modes depend little on the value of l. This is to be expected because the excitation and damping mechanisms are significant only very close to the surface, where the vertical scale is much less than the horizontal scale of oscillations and when l is low the modal inertia is quite insensitive to degree l. It is therefore adequate to simplify the calculations, by analysing only radial modes of oscillation. The results are applicable to all modes of moderately low degree.

2. Observational projects

Observations of oscillation properties of stars other than the Sun provide important information for testing the theory of stellar evolution. A critical problem with the detection of oscillations in solar-type stars, however, is their very small amplitudes, of the order of $1\,\mathrm{m\,s^{-1}}$ or less. For the Sun the observed velocity variations in disc-integrated light have values $\lesssim 20\,\mathrm{cm\,s^{-1}}$ (e.g. Grec et al. 1983; Libbrecht & Woodard 1991; Chaplin et al. 1998). To detect similar variations in distant stars is therefore a challenging task, requiring observations to be made with the utmost precision.

Three observing techniques for detecting such oscillations have been developed so far. The first is to search for periodic Doppler shifts of spectral lines (e.g. Kennelley 1995). However, the most successful result by this method has been the determination of only an upper bound to oscillation amplitudes in some of the brightest stars (e.g. Brown & Gilliland 1990; Brown et al. 1991; Mosser et al. 1998). The second method is to look for periodic brightness fluctuations using photometry. When used with area detectors such as CCDs, this method has a clear advantage over spectroscopic techniques because it permits one to observe large ensembles of stars simultaneously (e.g. Gilliland 1995). Using differential CCD photometry with seven 4m-class telescopes, Gilliland et al. (1993) obtained upper limits of luminosity amplitudes of possible oscillations in twelve stars in M67. The third method, introduced by Kjeldsen & Bedding (1995), measures temperature fluctuations induced by stellar oscillations via their effects on the equivalent width of the Balmer lines (Bedding et al. 1996). This technique has yielded a possible detection of solar-like oscillations in the sub-giant η Boo (Kjeldsen et al. 1995). Although it is currently restricted to observing isolated stars, the equivalent-width method is insensitive to atmospheric scintillation, and attains a substantially better signal-to-noise ratio than do the other two ground-based methods.

The limitations of ground-based observational techniques in asteroseismology have been addressed by Frandsen (1992) and Gilliland (1995), both of whom argued that seismology can be applied to distant solar-type stars only by observing them from space. The elimination of atmospheric noise and the possibility of obtaining long continuous data sequences will provide information of much higher quality than from any ground-based method. Several asteroseismological space projects are in preparation, such as the French project COROT[1] (Catala et al. 1995), the Danish project MONS[2] (Kjeldsen & Bedding 1998) and the Canadian project MOST[3] (Matthews 1998).

When preparing an observing campaign, it is helpful in the selection of target stars to have a good prediction of the amplitude of the signal one will be trying to observe. Measurements of mode lifetimes (damping rates) and the variation of oscillation amplitudes, which depend, in part, on stellar parameters, provide invaluable insights into the mechanisms that excite solar-like oscillations. It is hoped that future observations will provide these crucial measurements. The aim of this paper is to provide a systematic survey of the oscillation properties in view of these upcoming observational projects.

3. Time-dependent convection

In order to describe the turbulent fluxes in a time-dependent envelope, various phenomenological mixing-length models have been proposed (for a detailed discussion see Balmforth 1992a; Houdek 1996). In envelopes that do not pulsate, the various guises of local mixing-length method are essentially similar, once their intrinsic parameters have been calibrated (their formulations may be interpreted as providing interpolation formulae between the two limits of efficient and inefficient convection; Gough & Weiss 1976). This is not so of formulations of time-dependent mixing-length prescriptions, in which the details of the phenomenological model influence the predictions of stability (Balmforth 1992a). Moreover, local theories are plagued by some fundamental inconsistencies, which we shall describe presently. For these reasons, we prefer to use a nonlocal version (Gough 1976) which is summarized below.

[1] COnvection and ROTation
[2] Measuring Oscillations in Nearby Stars
[3] Microvariability & Oscillations of STars

3.1. Local mixing-length model

Local mixing-length models (e.g. Böhm-Vitense 1958; Ulrich 1970b; Gough 1977) still provide the almost universal method for computing the stratification of convection zones in stellar models. One of the major drawbacks of a local approach is the assumption that the characteristic length scale ℓ must be shorter than any scale associated with the structure of the star. This condition is certainly violated in solar-like stars and in red giants, where calibrated evolution calculations yield a typical value for the mixing-length parameter $\alpha = \ell/H_p$ that is of order unity, where H_p is the pressure scale height. (Since α is normally thought to be essentially invariable, it follows that the condition must be thought to be violated in all stars.) This implies that fluid properties vary significantly over the extent of a convective element; the superadiabatic gradient can vary on a scale much shorter than ℓ.

In many computations of stellar envelope models, the turbulent pressure $p_{\rm t}$ associated with the Reynolds stresses has been ignored. However, several investigations (Baker & Gough 1979; Rosenthal et al. 1995; Canuto & Christensen-Dalsgaard 1998) suggest that the momentum flux provides a substantial fraction of the hydrostatic support in the equilibrium model, and should therefore not be neglected. In a local model, inclusion of the momentum flux $p_{\rm t} = \rho w^2$ (ρ being the mean density and w the rms vertical velocity of the convective elements) leads to singular points in the equation for the turbulent pressure gradient at the edges of the convective regions (e.g. Gough 1976). This issue demands careful consideration, although it can be circumvented by adopting an additional approximation to reduce the order of the equations of hydrostatic support, which are then not strictly consistent with the formulation of the theory (Henyey, Vardya & Bodenheimer 1965; Baker & Gough 1979).

In a time-dependent description, the details of the phenomenological model become important to the linear stability calculation; the nonlocal model that we employ in our calculations is one that is based on Gough's (1965, 1977) local mixing-length model. In that formulation, the turbulent eddies that support the heat and momentum fluxes evolve in a pulsating environment. Explicit consideration is given to the phase of pulsation at the birth of each transitorily coherent eddy, and to how the eddy adjusts to the temporally varying environment. Other mixing-length models (e.g. Unno 1967, Xiong 1989) emphasize other aspects of the dynamics, which presumably influence differently the pulsational stability (Balmforth 1992a).

Another major drawback of local theory is that it fails to treat the convective dynamics across extended eddies in a physically plausible fashion: in deeper parts of the convection zone, where the stratification is almost adiabatic, convective heat transport is very efficacious; radiative diffusion is unimportant, and the perturbation of the heat flux is dominated by advection of temperature fluctuations. In this limit, the temperature fluctuation can be described approximately by a diffusion equation in which the diffusivity is imaginary (Baker & Gough 1979; Gonczi & Osaki 1980). Rapid spatial oscillations of the eigenfunctions result. The problem this introduces can at best be thought of as one of numerical resolution, which is particularly severe in layers where the stratification is very close to being adiabatic. But worse, it signifies a complete failure of the model, since the wavelength of the spatial oscillation is very much smaller than the mixing length (which is supposedly the smallest lengthscale permitted by the model).

3.2. Nonlocal mixing-length model

The obvious drawbacks of a local formulation of the mixing-length approach can be removed by an appropriate nonlocal generalization. Account can be taken of the finite size of a convective eddy by averaging spatially the representative value of a physical variable throughout the eddy. Spiegel (1963), for example, proposed a nonlocal description based on the concept of an eddy phase space, and derived an equation for the convective flux which is similar to a radiative-transfer equation. The solution of this transfer equation yields an integral expression that converts the usual ordinary differential equations describing stellar models into integro-differential equations. The solution to the transfer equation can be approximated by taking moments, closing the hierarchy at second order with the Eddington approximation (Gough 1976). In this approximation, the nonlocal generalization of the mixing-length formulation is governed by three second-order differential equations for the spatially averaged convective fluxes $F_{\rm c}$ and $p_{\rm t}$ and for the average superadiabatic temperature gradient experienced by an eddy.

The procedure introduces two more parameters, a and b, which characterize respectively the spatial coherence of the ensemble of eddies contributing to the total heat and momentum fluxes, and the extent over which the turbulent eddies experience an average of the local stratification. Theory suggests approximate values for these parameters, but it is arguably better to treat them as free. Roughly speaking, the parameters control the degree of "nonlocality" of convection; low values imply highly nonlocal solutions, and in the limit $a, b \to \infty$ the system of equations reduces to the local formulation (except near the boundaries of the convection zone, where the equations are singular). Balmforth (1992a) investigated the effect of the parameters a and b on the turbulent fluxes in the solar case, and Tooth & Gough (1989) tried to calibrate a and b by comparing theory with laboratory experiments.

4. Model computations

The basic model calculations reported in this paper are as described by Balmforth (1992a). In particular, we incorporate turbulent pressure in the equilibrium model envelope. The computation proceeds by iteration, from a trial solution obtained by integrating inwards from an optical depth of $\tau = 10^{-4}$ and ending at a radius fraction 0.2, using local mixing-length theory and the diffusion approximation to radiative transfer; the approximation to the turbulent pressure used by Baker & Gough (1979) is adopted to obviate singular points at the edges of the convection zones. The entire envelope is then re-integrated using

the equations appropriate to the nonlocal mixing-length theory, using the Eddington approximation to radiative transfer (Unno & Spiegel 1966). The atmosphere is treated as being grey, and is assumed to be plane parallel. The temperature gradient is corrected by using a τ-dependent varying Eddington factor (Auer & Mihalas 1970) derived from model C of Vernazza et al. (1981) in the manner of Balmforth (1992a). Opacities were obtained from the latest OPAL tables (Iglesias & Rogers 1996), supplemented at low temperature by tables from Kurucz (1991). Interpolation in these tables was carried out using birational splines (Houdek & Rogl 1996). The equation of state included a detailed treatment of the ionization of C, N, and O, and a treatment of the first ionization of the next seven most abundant elements (Christensen-Dalsgaard 1982), as well as 'pressure ionization' by the method of Eggleton, Faulkner & Flannery (1973); electrons were treated with relativistic Fermi-Dirac statistics. In the pulsation model the boundary conditions used are essentially those of Baker & Kippenhahn (1965), but supplemented by appropriate conditions on the variables of the nonlocal mixing-length theory (Balmforth 1992a). The outer boundary conditions were applied at the temperature minimum, the mechanical condition being consistent with a perfectly reflecting surface; at the base of the envelope, conditions of adiabaticity and vanishing displacement were imposed.

The linearized pulsation equations were solved with a second-order accuracy Newton-Raphson-Kantorovich algorithm (Baker, Moore & Spiegel 1971; Gough, Spiegel & Toomre 1974). With this algorithm the eigenfunctions and eigenvalues can be computed simultaneously; however, one has to provide a proper trial solution. This can be obtained by solving first the adiabatic pulsation equations and then applying a quasi-adiabatic approximation[4] to complete the nonadiabatic system. The detailed equations describing the equilibrium and pulsation model have been discussed by Balmforth (1992a) and Houdek (1996).

5. Damping rates

Were solar p modes to be genuinely linear and stable, their power spectrum could be described in terms of an ensemble of intrinsically damped, stochastically driven, simple-harmonic oscillators (Batchelor 1956; Christensen-Dalsgaard et al. 1989) provided the background equilibrium state of the star is independent of time; if we further assume that mode phase fluctuations contribute negligibly to the width of the spectral lines, the intrinsic damping rates of the modes could then be determined observationally from measurements of the pulsation linewidths. The linewidths are obtained, to a first approximation, by fitting Lorentzian profile functions to the spectral peaks of the observed power spectrum. Higher approximations demand a more detailed description of the excitation and damping (cf. Jefferies et al. 1988; Gabriel 1998). Continuous observations over many periods are required. Observations from GONG (Harvey et al. 1996), and from the SOI-MDI (Scherrer et al. 1991), VIRGO (Fröhlich et al. 1995) and GOLF (Gabriel et al. 1991) instruments aboard the SOHO spacecraft have already provided such high-quality data for the Sun.

It should be noted that the observed power spectrum of solar pulsations is complicated by the beating of closely spaced modes (e.g. Christensen-Dalsgaard & Gough 1982; Hill et al. 1996) and by amplitude variations and phase wandering resulting from the interaction with the turbulent convection. These effects might also be responsible for the observed asymmetries in the p-mode line profiles. The study of how to disentangle the manifestations of these phenomena from manifestations of the intrinsic mode parameters is only in its infancy (Chang et al. 1997; Roxburgh & Vorontsov 1997; Gabriel 1998; Nigam et al. 1998; Rast & Bogdan 1998). It is important for analysing not only the oscillations of the Sun, but the oscillations of any star with a rich spectrum of frequencies.

5.1. Processes contributing to intrinsic linewidths

Basically, the damping of stellar oscillations arises from two sources: processes influencing the momentum balance, and processes influencing the thermal energy equation. Each of these contributions can be divided further according to their physical origin, as illustrated in Fig. 1. A detailed discussion of the processes has been given by Houdek (1996). Here we limit the discussion to those that are modelled in our computations.

Nonadiabatic radiative processes can contribute to both the driving and the damping of the pulsations. In solar-type stars the zones of ionization lie well inside the regions of efficacious convection, and the conventional κ-mechanism provides only a relatively small contribution to the driving. Radiative damping in the atmosphere is not necessarily small, and requires a more accurate treatment of radiative transfer than the diffusion approximation. Christensen-Dalsgaard & Frandsen (1983a) have shown that the use of the grey Eddington approximation, when applied correctly, does not introduce too large an error in the calculation of the damping rates. Furthermore, they have demonstrated that for stability calculations departures from radiative equilibrium in the mean state must not be neglected: in the upper boundary layer of the convection zone, where there is a transition from convective to radiative energy transport, radiative equilibrium is no longer maintained. Thus the mean intensity J is not equal to the Planck function B. In particular, by perturbing the equations describing the radiation field in the Eddington approximation, one obtains (Christensen-Dalsgaard & Frandsen 1983a)

$$\delta\left(\frac{1}{\rho}\mathrm{div}\,\boldsymbol{F}_{\mathrm{r}}\right) = 4\pi\kappa\left[\delta B - \delta J + \frac{\delta\kappa}{\kappa}(B_0 - J_0)\right] , \qquad (1)$$

where ρ and κ denote the density and opacity, respectively, the operator δ denotes a Lagrangian perturbation, and the subscript 0 denotes an equilibrium quantity. The last term in Eq. (1) describes the departure from radiative equilibrium in the mean state; it is not everywhere small, yet it has been ignored in most stability calculations so far.

[4] Quasi-adiabatic approximations adopt adiabatic eigenfunctions for evaluating the thermal variables for computing mode stability.

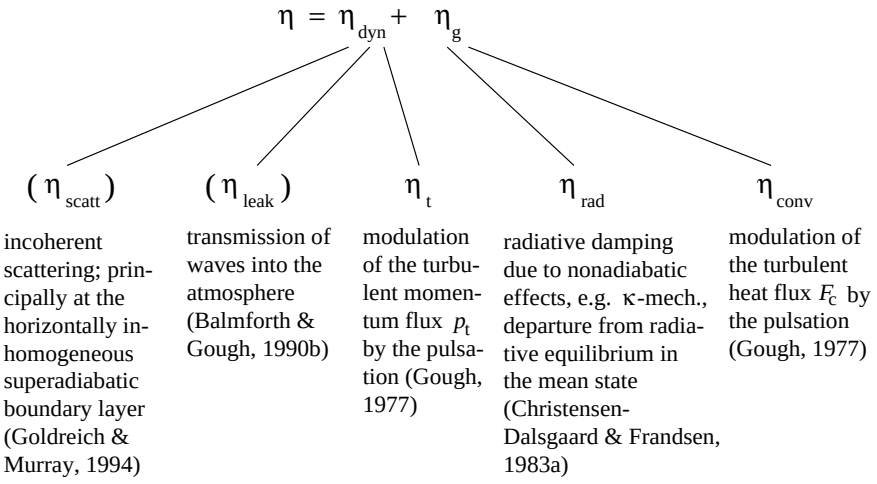

Fig. 1. Physical processes contributing to the linear damping rate η. They can be associated with the effects arising from the momentum balance ($\eta_{\rm dyn}$) and from the thermal energy balance ($\eta_{\rm g}$). The contributions $\eta_{\rm scatt}$ and $\eta_{\rm leak}$ are in parentheses because they have not been taken into account in the computations reported in this paper. The influence of Reynolds stresses on solar modes, contributing to $\eta_{\rm t}$, has been treated by Goldreich & Keeley (1977a) in the manner of a time-independent scalar turbulent viscosity. The width of the line in the Fourier power spectrum of the oscillations is influenced also by nonlinearities, both those coupling a mode to others (Kumar & Goldreich, 1989) and those intrinsic to the mode itself.

Vibrational stability is influenced further by the exchange of energy between the pulsation and the turbulent velocity field. The exchange arises either via the pulsationally perturbed convective heat flux, or directly through dynamical effects of the fluctuating Reynolds stresses. In fact, it is the modulation of the turbulent fluxes by the pulsations that seems to be the predominant mechanism responsible for the driving and damping of solar-type acoustic modes.

Nonadiabatic processes attributed to the modulation of the convective heat flux by the pulsation are accounted for by the contribution $\eta_{\rm conv}$ to the total damping rates (see Fig. 1). This contribution is related to the way that convection modulates large-scale temperature perturbations induced by the pulsations, which influences pulsational stability substantially. The manner in which it does so, together with the conventional κ-mechanism, is discussed by Balmforth (1992a). It appears to have a significant destabilizing influence on the pulsations (Balmforth & Gough 1990a).

It was first reported by Gough (1980) that the dynamical effects arising from the turbulent momentum flux perturbations $\delta p_{\rm t}$ contribute significantly to the damping $\eta_{\rm t}$. Detailed analyses (Balmforth 1992a) reveal how damping is controlled largely by the phase difference between the turbulent pressure perturbation $\delta p_{\rm t}$ and the density perturbation $\delta\rho$. Turbulent pressure fluctuations must not, therefore, be neglected in stability analyses of solar-type p modes.

The results presented here were obtained from computations including the physics describing $\eta_{\rm rad}$, $\eta_{\rm conv}$ and $\eta_{\rm t}$. The nonadiabatic contributions $\eta_{\rm rad}$ and $\eta_{\rm conv}$ may be associated with the thermodynamics of the gas, and accordingly we couple them into $\eta_{\rm g} = \eta_{\rm rad} + \eta_{\rm conv}$ (see also Fig. 1).

5.2. Theoretical damping rates

Damping rates are computed as the imaginary part $\omega_{\rm i}$ of the complex eigenfrequency $\omega = \omega_{\rm r} + {\rm i}\,\omega_{\rm i}$, obtained from solving the fully nonadiabatic pulsation equations. Balmforth (1992a) computed damping rates for the Sun, and reported that he found all modes to be stable, with damping rates agreeing tolerably with observation for frequencies between 2 mHz and 4 mHz. Below and above this frequency range the theoretical damping rates are smaller than observations would suggest. Damping arising from incoherent scattering $\eta_{\rm scatt}$ (Goldreich & Murray 1994, see Fig. 1), which may remove the discrepancy both at low and at high frequencies, is not modelled in our calculations.

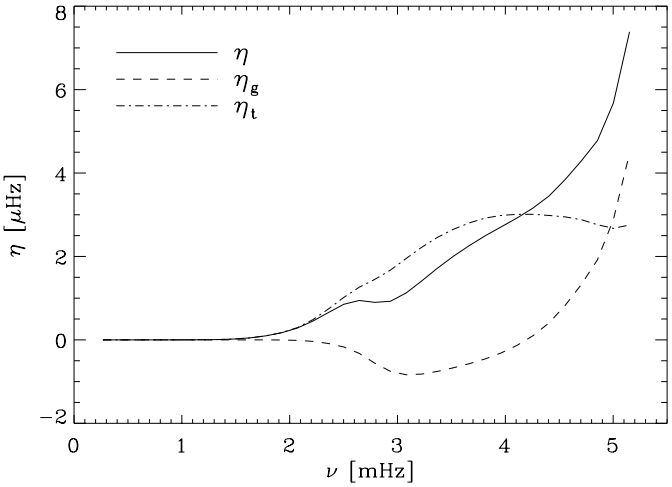

Fig. 2. Linear damping rates η for the Sun as function of frequency. The values chosen for the convection parameters are $\alpha = 1.8$ and $a^2 = b^2 = 600$.

Fig. 2 displays the damping rates and their contributions arising from the gas and turbulent pressure perturbations for a solar envelope model. Damping is much augmented by the turbulent pressure perturbation $\delta p_{\rm t}$; it is only at the highest frequencies that the nonadiabatic contribution $\eta_{\rm g}$ to damping of solar p modes exceeds that from the turbulent pressure $\eta_{\rm t}$.

The total damping rate η (solid curve), plotted as a function of cyclic frequency $\nu = \omega_{\rm r}/2\pi$, is characteristically flat at frequencies near 2.8 mHz (see Fig. 2). This feature is also observed in solar linewidth measurements (e.g. Libbrecht 1988, Appourchaux et al. 1998, Chaplin et al. 1998). At these frequencies the net damping is reduced particularly by radiative processes

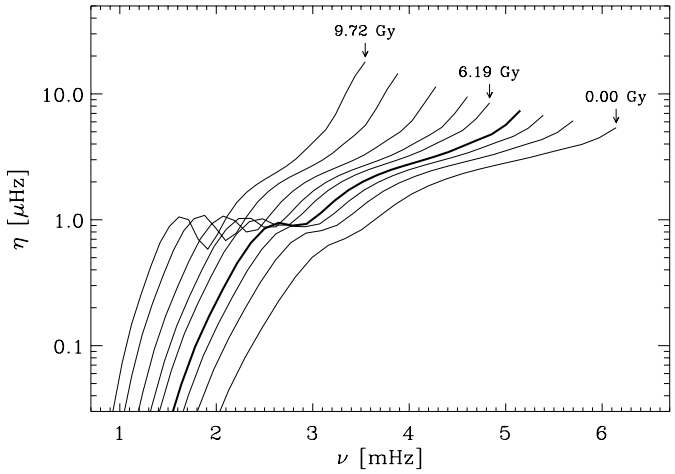

Fig. 3. Damping rates for an evolving $1\,M_\odot$ star as function of frequency. The results are displayed for models with ages=(0, 2.49, 3.96, 4.55, 6.19, 7.00, 8.03, 9.02, 9.72) Gy. The thick curve indicates the results for the present Sun. Values $\alpha = 1.8, a^2 = b^2 = 600$ for the convection parameters have been used.

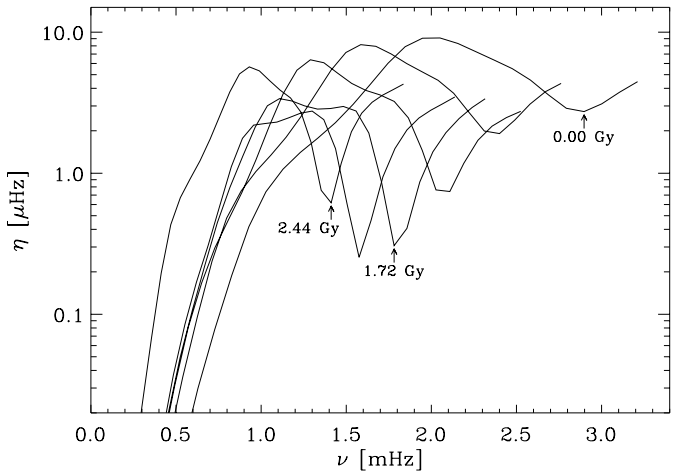

Fig. 4. Damping rates for an evolving $1.45\,M_\odot$ star as a function of frequency. The results are depicted for models with ages=(0, 0.96, 1.38, 1.72, 2.00, 2.44) Gy. Values $\alpha = 2.0, a^2 = 900, b^2 = 2000$ for the convection parameters have been used.

in the upper superadiabatic boundary layer of the convection zone, which are locally destabilizing.

The damping rates for an evolving $1\,M_\odot$ star are depicted in Fig. 3. Damping rates generally increase with increasing age, particularly for low- and high-order modes. For modes of intermediate order the flattening of the damping-rate curve becomes more pronounced as the star evolves, and turns into a locally concave function at about the solar age. The maximum value of the superadiabatic temperature gradient of a $1\,M_\odot$ star increases by approximately 24% along the main sequence, promoting the depression in the damping rates.

A similar behaviour of the damping rates is obtained for more massive stars, as indicated for the evolving $1.45\,M_\odot$ star depicted in Fig. 4. For these more massive stars, larger values of the nonlocality parameters, $a^2 = 900$ and $b^2 = 2000$, were

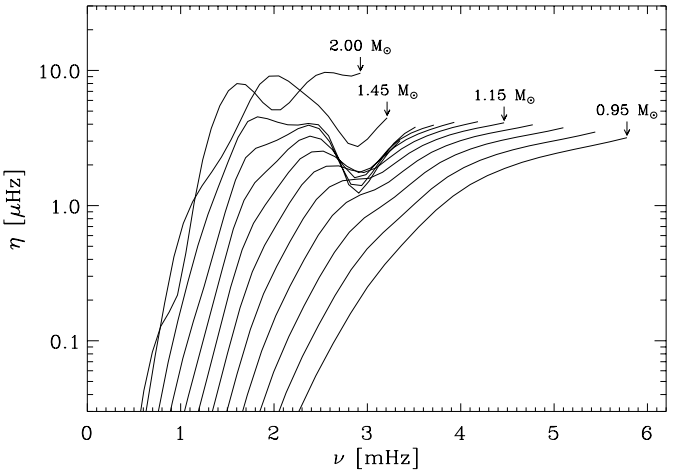

Fig. 5. Damping rates for ZAMS models as functions of frequency. The results are displayed for models with M=(0.95, 1.00, 1.05, 1.10, 1.15, 1.20, 1.25, 1.30, 1.35, 1.40, 1.45, 2.00) $M_\odot$. For the convection parameters the values $\alpha = 2.0, a^2 = 900, b^2 = 2000$ have been used.

adopted. This selection ensured that all the radial modes were stable, in line with our working hypothesis that stochastic excitation underlies the appearance of solar-like oscillations (but see Sect. 9). The depression in the damping rates is more pronounced for these stars, even at the ZAMS. This trend may be seen even more obviously in Fig. 5, where damping rates are depicted for stars with increasing mass along the ZAMS.

The functional dependence of η on stellar parameters was determined approximately by Goldreich & Kumar (1991); they derived an order-of-magnitude estimate for the damping rates accounting roughly for the effects of radiative damping and convective dynamics. The radial modes were treated in the polytropic approximation to the outer layers and convection was described by standard (unperturbed) local mixing-length theory (Böhm-Vitense 1958). They obtained the expression

$$\eta \sim \frac{L}{c_{\rm s}^2 I_\omega}\left(\frac{\omega_{\rm r}}{\omega_{\rm c}}\right)^2 , \tag{2}$$

where L is the luminosity and $c_{\rm s}$ denotes the adiabatic sound speed at the photosphere (which we define at the level where the temperature is equal to the effective temperature), I_ω is the mode inertia, and $\omega_{\rm c}$ is the acoustical cut-off frequency in an isothermal atmosphere (Lamb 1909),

$$\omega_{\rm c} = \frac{c}{2H_p} , \tag{3}$$

where c denotes the sound speed. The inertia is usually defined such that it represents the coefficient of proportionality between the energy in the mode and the square of the velocity amplitude of the associated disturbance in the surface layers of the star. The surface of the star, however, commonly lies in a region where the mode is evanescent, and in that case I_ω is more usefully regarded as a measure of evanescence, representing a property of the eigenfunction above the upper turning point (Gough 1995). For the case of a linear adiabatic mode of stellar oscillation, which can be represented by an undamped harmonic oscillator,

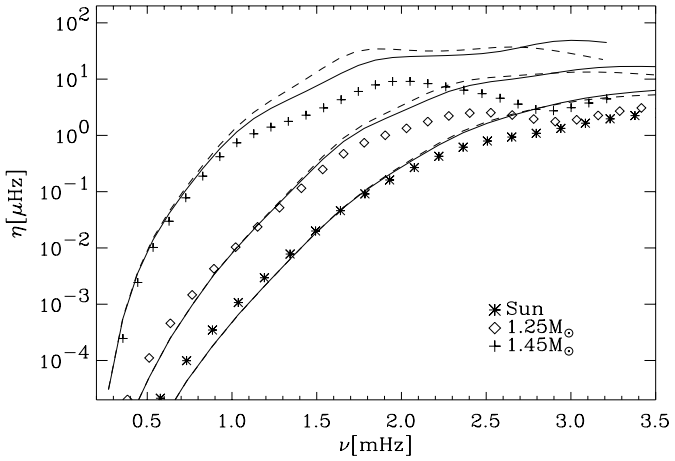

Fig. 6. Theoretical damping rates as functions of frequency for the Sun, a $1.25\,M_\odot$ and a $1.45\,M_\odot$ ZAMS star. The curves are the right-hand side of expression (2) multiplied by the factor $1/6$, assuming adiabatically (dashed curves) and nonadiabatically (solid curves) computed mode inertia I_ω. The symbols show the damping rates obtained directly from the corresponding pulsation calculations, in which were solved the fully nonadiabatic linearized equations using the nonlocal, time-dependent mixing-length model with the convection parameters of Figs 4 and 5.

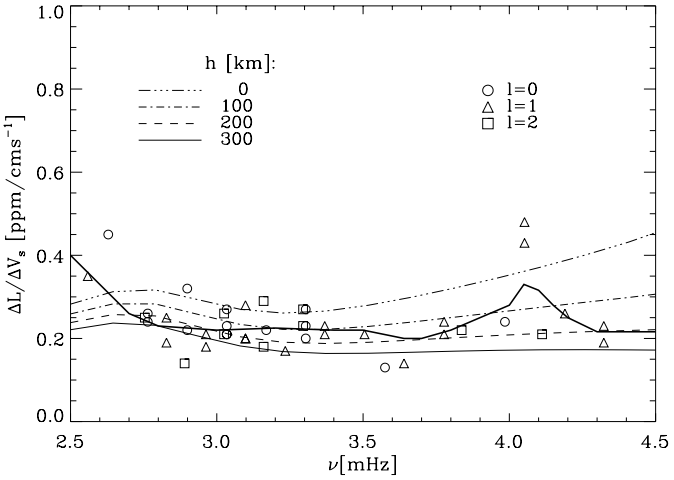

Fig. 7. Theoretical amplitude ratios for a solar model compared with observations by Schrijver et al. (1991). Computed results are depicted for velocity amplitudes obtained at different heights above the photosphere ($h = 0$ km at $T = T_{\rm eff}$) assuming the convection parameters used for Figs 2 and 3. The thick, solid curve indicates a running-mean average of the data.

the mode inertia I_ω can be defined in terms of the total (kinetic + potential) energy E and the mean-square value of its surface velocity $V_{\rm s}$, i.e., $E = I_\omega\, V_{\rm s}^2$, and consequently

$$I_\omega = \frac{1}{\xi^2(R_\star)} \int_{m_{\rm b}}^{M_\star} |\xi(m,\omega_{\rm r})|^2 \,{\rm d}m\,. \tag{4}$$

Here $m_{\rm b}$ denotes the mass interior to the bottom boundary of the envelope, and $R_\star$ and $M_\star$ represent respectively the radius and the mass of the star. In practice, we normalize the eigenfunction $\xi(m,\omega_{\rm r})$ such that

$$\frac{\xi(R_\star)}{R_\star} = 1\,. \tag{5}$$

In Fig. 6 we compare numerically computed damping rates with estimates from expression (2) with the right-hand side multiplied (arbitrarily) by 1/6. The factor 1/6 can be obtained approximately by taking into account the adiabatic exponents (γ_1 and γ_3) in the derivation of expression (2), assuming a fully ionized gas. For the mode inertia I_ω (cf. Eq. 4) the calculations assumed adiabatically (dashed curves) and nonadiabatically (solid curves) computed displacement eigenfunctions ξ.

For frequencies below about half the isothermal acoustical cut-off frequency $\omega_{\rm c}$, the results suggest a fair agreement between analytical and modelled damping rates. An interesting feature is the bend in the analytical solution obtained with both the nonadiabatic and adiabatic eigenfunctions for the $1.45\,M_\odot$ star near the frequency $\nu \simeq 1.85$ mHz. This property is obviously related to the shape of the eigenfunctions in the boundary layers of the convection zone, because in a polytrope the mode inertia I_ω is a smooth function of height (Gough 1995). The characteristic flattening of the damping rates (e.g., near 2.8 mHz for the Sun), however, is not seen in the estimates from expression (2).

6. Amplitude ratios

A useful test of the pulsation theory, independent of an excitation model, is provided by comparing estimated intensity-velocity amplitude ratios with observations. For the Sun, accurate irradiance measurements exist from the IPHIR instrument of the PHOBOS 2 spacecraft with contemporaneous low-degree velocity observations in the potassium line from the Birmingham instrument at Tenerife (Schrijver et al. 1991). This allows us to compare observed solar amplitude ratios with our estimated ratios as function of frequency. The comparison is displayed in Fig. 7, where the model results are depicted for velocity amplitudes computed at different atmospheric levels. For moderate and high eigenfrequencies the amplitude of the displacement ξ increases quite steeply in the evanescent outer region of the atmosphere, where the density declines very rapidly. The computed velocity amplitude, and hence the ratio, varies by about 15 % between the photosphere and the temperature minimum. Thus attention has to be paid to which atmospheric level the velocity amplitudes are computed, i.e., at which level the displacement eigenfunctions are normalized. Observations are performed in selected Fraunhofer lines, e.g. in the neutral potassium line (769.9 nm) as used in the BiSON observation (Elsworth et al. 1993), which is formed at a height of $h \simeq 200$ km above the point where the temperature is equal to the effective temperature (assuming the T-τ relation derived from the model C atmosphere of Vernazza et al. 1981). The luminosity amplitudes have been computed at the outermost gridpoint and a correction factor has been applied to account for the conversion to the measured irradiance wavelength of $\lambda = 500$ nm using the approximation of Kjeldsen & Bedding (1995). Observations with

a coherence greater than 0.7 are represented by different symbols denoting measurements of different degree l. The thick solid curve represents a running-mean average, with a width of $300\,\mu$Hz, of the observational data. The theoretical ratios for $h = 200\,$km (dashed curve) show reasonable agreement with the observations.

7. Acoustical noise generation rate

Acoustical radiation by turbulent multipole sources in the context of stellar aerodynamics has been considered by Unno & Kato (1962), Moore & Spiegel (1964), Unno (1964), Stein (1967), Goldreich & Keeley (1977b), Osaki (1990), Balmforth (1992b), Goldreich et al. (1994) and Musielak et al. (1994).

In a pulsating atmosphere the full pulsation-convection equations must be derived from the fluid-dynamical equations in which the fluid velocity includes both turbulence and pulsation. Balmforth (1992b) reviewed the theory of acoustical excitation in a pulsating atmosphere, and, following Goldreich & Keeley (1977b), he derived the following expression for the rate of energy injected into a mode with frequency $\omega_{\rm r}$ by quadrupole emission through the fluctuating Reynolds stresses:

$$P_{\rm Q} = \frac{\pi^{1/2}}{8 I_\omega \xi^2(R_\star)} \times \int_{M_*} \left(\frac{\partial \xi(m,\omega_{\rm r})}{\partial r} \right)^2 \rho \ell_0^3 u_0^4 \tau_0 \mathcal{S}(m,\omega_{\rm r})\,{\rm d}m\,, \qquad (6)$$

where ℓ_0,u_0,τ_0 are respectively the length, velocity and correlation time scales of the most energetic eddies, determined by the mixing-length model. The function $\mathcal{S}(m,\omega_{\rm r})$ accounts for the turbulent spectrum, which approximately describes contributions from eddies with different sizes to the noise generation rate $P_{\rm Q}$, and which we implemented as did Balmforth (1992b):

$$\mathcal{S}(m,\omega_{\rm r}) = \int_0^\infty \frac{u_\kappa^3}{\kappa^5} \exp[-\omega_{\rm r}^2 \tau_0^2/(2\kappa u_\kappa)^2]\,{\rm d}\kappa\,, \qquad (7)$$

where $\kappa = k/k_0$, $u_\kappa = u(k)/u_0$, k is the wavenumber of an eddy with velocity $u(k)$, and k_0 is the wavenumber at the peak of the spectrum. For the computation of $u(k)$, a turbulent spectrum according to Spiegel (1962) has been chosen.

The emission of acoustical radiation by turbulent multipole sources depends critically on the convective velocity u. In homogeneous isotropic and non-decaying turbulence, acoustic emission by the fluctuating Reynolds stresses (quadrupole emission) scales with the fifth power of the turbulent Mach number $M_{\rm t} = u/c$ (Lighthill-Proudman formula). Inhomogeneity and anisotropy effects in the overturning layers of stars give rise to monopole and dipole emission manifested in the fluctuation of the entropy (e.g. Goldreich & Kumar 1990). Stein & Nordlund (1991) and Goldreich et al. (1994) suggest that the monopole and dipole source may be as important as quadrupole radiation. However, previous work has demonstrated that the prescription is capable of roughly reproducing solar measurements, and so, partly for want of a serious theory, we stick with the expressions (6) and (7) here.

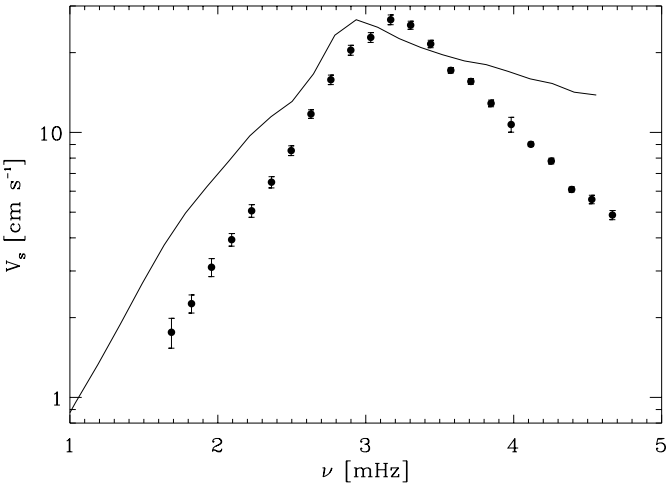

Fig. 8. Velocity amplitudes for the Sun as a function of frequency. The computed values (continuous curve) are depicted at the photospheric level $h = 200\,$km. The turbulent spectrum $\mathcal{S}(m,\omega_r)$, given by Eq. (7), has been multiplied by the factor 6.55 to fit the maximum value of the velocity data (filled circles) from the BiSON observations (Chaplin et al. 1998). The data are from a 32-month almost continuous sequence collected between May 1994 and January 1997, i.e., at or near the solar-cycle 22/23 activity minimum. The computations assumed the convection parameters $\alpha = 1.8, a^2 = b^2 = 300$.

8. Amplitudes

8.1. Velocity amplitudes

With the computations of the damping rate, η, and noise generation rate, $P_{\rm Q}$, the root-mean-square velocity at a particular level in the atmosphere may be written as

$$V_{\rm s} = \sqrt{\frac{P_{\rm Q}}{2\,\eta\,I_\omega}}\,. \qquad (8)$$

The form of the turbulent spectrum $\mathcal{S}(m,\omega_{\rm r})$, given by Eq. (7), has a substantial effect on the predicted mode amplitudes. In this paper we multiplied the rhs of Eq. (7) by the factor 6.55 for all amplitude predictions. This empirical correction, which can be attributed perhaps to uncertainties in our expressions for the quadrupole emission, leads to theoretical solar velocity amplitudes that have the same maximum value of 26.6 cm s^{-1} as that observed by the BiSON group (Chaplin et al. 1998). The results of the scaled theoretical mean amplitude values for a solar model are displayed in Fig. 8 together with the BiSON data.

8.1.1. Main-sequence stars

The mean velocity as a function of frequency, computed at a height $h = 200\,$km above the photosphere of an evolving $1\,M_\odot$ star, is displayed in Fig. 9. The oscillation amplitudes become larger with age for low and intermediate frequencies, exhibiting a maximum value of $V_{\rm s} \simeq 45\,$cm s^{-1} at the end of the hydrogen core-burning phase. The increase comes about because the ratio $P_{\rm Q}/I_\omega$ increases with age at the frequency of maximum mode

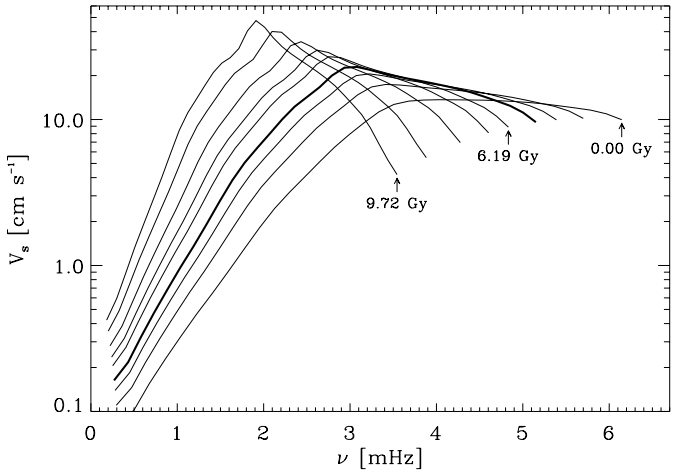

Fig. 9. Velocity amplitudes for an evolving $1\,M_\odot$ star as function of frequency, depicted at the photospheric level $h = 200$ km. The results are displayed for the model masses and convection parameters of Fig. 3. The thick curve indicates the results for the Sun.

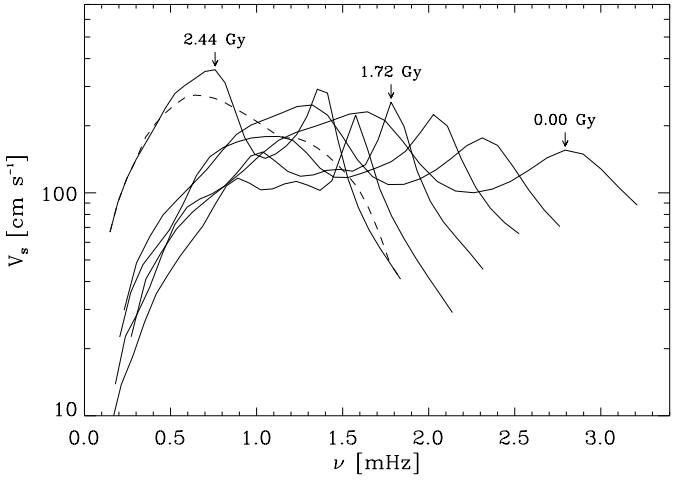

Fig. 10. Velocity amplitudes for an evolving $1.45\,M_\odot$ star as function of frequency, computed at a height $h = 200$ km. The dashed curve displays the result for the 2.44 Gy model applying a median filter on the amplitudes with a width corresponding to nine radial modes. The amplitudes are portrayed for the model ages and convection parameters of Fig. 4.

energy, whereas the damping rates decrease with age at this frequency (see Fig. 3).

In Fig. 10 the amplitudes are depicted for an evolving $1.45\,M_\odot$ star, also computed at the height $h = 200$ km. For models before the characteristic 'hook' (i.e., at ages $\lesssim 2.36$ Gy) in the evolutionary track (see Fig. 13) the amplitudes increase only moderately with age, mainly because of the increasing mode inertia at the frequency of maximum mode energy and the consequent decrease of the ratio $P_{\rm Q}/I_\omega$. For models older than ~ 2.36 Gy, the luminosity increases fairly rapidly, leading to a steep increase in the turbulent Mach number and hence in the noise generation rate $P_{\rm Q}$, and consequently mode amplitudes. Near the end of the hydrogen core-burning phase the theory predicts maximum values of ~ 330 cm s^{-1} for the velocity amplitudes. In general these maximum values coincide with the sharp depression in the damping rates (see Fig. 4).

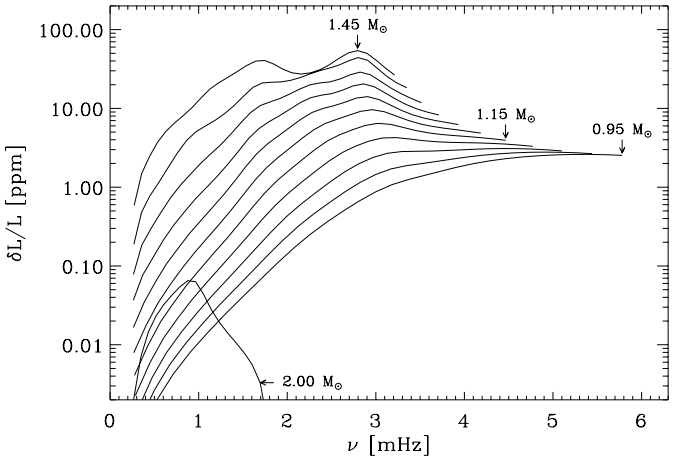

Fig. 11. Luminosity amplitudes for ZAMS model as function of frequency, displayed at the outermost meshpoint of the models. The computations assumed the convection parameters and model masses of Fig. 5.

8.2. Luminosity amplitudes

For radial modes, the imaginary part of the nonadiabatic displacement eigenfunctions is very small relative to the real part. The differences in the velocity amplitudes when using the adiabatic instead of the nonadiabatic displacement eigenfunctions are negligible relative to the uncertainties inherent in modelling the theory of stochastic excitation. For the estimation of the luminosity amplitudes, however, nonadiabatic eigenfunctions of the relative luminosity fluctuations, $\delta L/L_0$, have to be taken into account. The relative luminosity amplitudes are related linearly to the velocity amplitudes.

8.2.1. Zero-age main-sequence stars

The luminosity amplitudes of moderate-mass stars along the ZAMS are depicted in Fig. 11. The amplitudes increase monotonically with M for stars with $M \leq 1.45\,M_\odot$, up to a maximum value of ~ 50 ppm. For models with $M \gtrsim 1.6\,M_\odot$, amplitudes of stochastically excited modes decrease with M; for a $2\,M_\odot$ ZAMS star the maximum amplitude is ~ 0.06 ppm. The dependence of the amplitude variations upon mass, or upon luminosity, may be explained principally by the strong dependence of the acoustic noise generation rate on the turbulent Mach number $M_{\rm t}$. The dependence of the maximum values of the turbulent Mach number $M_{\rm t}$ and the ratio of turbulent pressure to total pressure $p_{\rm t}/p$ upon model mass along the ZAMS is illustrated in Fig. 12. The computations predict the largest turbulent Mach numbers for models with a mass of $\sim 1.6\,M_\odot$. The $2\,M_\odot$ ZAMS star exhibits two very thin convection zones in the outer part of the envelope, and the theory predicts a maximum turbulent Mach number $M_{\rm t} < 0.1$. Furthermore, the opacity and consequently the convective heat flux decrease with M for

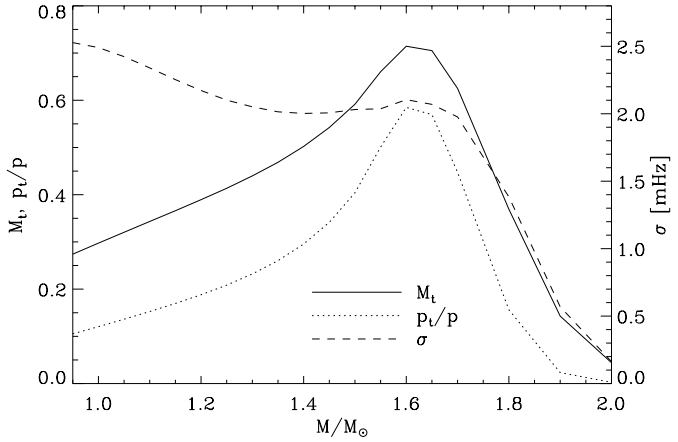

Fig. 12. Maximum values of turbulent Mach number $M_{\rm t}$, turbulent pressure fraction $p_{\rm t}/p$ and convective growth rate $\sigma = 2w/\ell$ as function of model mass along the ZAMS. The computations assumed the convection parameters of Figs 4 and 5.

$M \gtrsim 1.6\,M_\odot$. Also indicated in Fig. 12 is the maximum value of the convective growth rate $\sigma = 2w/\ell$, scaled in units of cyclic frequency ν. The ratio σ/ν influences the shape of the eigenfunctions in such a way as to cause a local depression in the damping rates η considered as functions of ν (cf. Gough 1997). The maximum value of σ is roughly equal to the frequency of the local minimum of η.

8.3. Dependence on stellar parameters

For those models on the main sequence for which all the modes are predicted to be stable, the computed maximum velocity amplitudes of stochastically excited modes (evaluated at the height $h = 200\,$km) are shown as contours on the HR diagram in Fig. 13. The 191 models (indicated by the diamond symbols) were generated by specifying the mass, luminosity and effective temperature provided from full evolution sequences, as obtained by Christensen-Dalsgaard (1993). The same convective parameters as those in Figs 4 and 5 were adopted. For more massive stars the maximum amplitudes exhibit peaks in their frequency spectrum due to the sharp dip in their damping rates (see Figs 4 and 10). We moderated these peaks by applying a median filter to the amplitudes of all models with a width in frequency corresponding to nine radial modes (as illustrated in Fig. 10 by the dashed curve for a $1.45\,M_\odot$ star with an age of $2.44\,$Gy).

The low-temperature extremities of the contours indicate where the model hydrogen mass fractions $X_{\rm c}$ reach 10^{-6} in the core; no calculations were carried out at lower temperatures. The amplitudes increase steeply with luminosity, particularly for stars with mass $M \gtrsim 1.4\,M_\odot$, owing to the increase in the convective velocities with M. The largest amplitudes are predicted for a $1.6\,M_\odot$ model of spectral type F2, which has a maximum velocity amplitude of ~ 15 times larger than that found for the Sun. For this model the turbulent Mach number is also predicted to be largest (see Fig. 12). For more massive stars the computations predict overstable modes (see Sect. 9). Amplitudes of such overstable modes are limited by nonlinear processes and can therefore not be estimated with the linear computations adopted in this paper; their values could be much larger than the amplitude values of the stable stochastically driven modes considered here.

For stars with $L \lesssim 2\,L_\odot$, the velocity amplitudes of stochastically excited modes depend strongly on the model luminosity and are only weakly dependent on the effective temperature. The same trend is also seen in Fig. 14 for the luminosity amplitudes (top panel). In the lower panel of Fig. 14 the ratios between luminosity and velocity amplitudes, $\Delta L/\Delta V_{\rm s}$, are displayed, where the luminosity fluctuations, ΔL, are computed at the outermost meshpoint of the models. At the photospheric level ($h = 0\,$km) the amplitude ratios appear to be quite insensitive to luminosity, and depend mainly on effective temperature.

Based on the model results of Christensen-Dalsgaard & Frandsen (1983b), Kjeldsen & Bedding (1995) proposed a scaling relationship for solar-type velocity amplitudes as a function of parameters used in stellar-evolution theory. In particular, they proposed the scaling law

$$\frac{V}{V_\odot} \sim \left(\frac{L/L_\odot}{M/M_\odot}\right)^s, \tag{9}$$

with $s = 1$, suggesting that the velocity amplitudes scale directly with the light-to-mass ratio L/M of the star. In Fig. 15 the velocity amplitudes versus the light-to-mass ratio are displayed at a height $h = 200\,$km above the photosphere for model calculations assuming the convection parameters of Fig. 4. There is a fair agreement between the computed amplitudes (filled circles) and Kjeldsen & Bedding's proposed relation (dashed line) for $L/M \lesssim 3$. For higher values of L/M the estimated amplitudes are predicted to be larger than Kjeldsen & Bedding's linear relation, particularly for models with masses $M/M_\odot \gtrsim 1.4$. Moreover, for these models the computed amplitudes become progressively more dependent on the model's effective temperature and less dependent on L/M as they evolve along their evolutionary tracks (see also Fig. 13). Applying a linear polynomial fit to the estimated amplitudes in Fig. 15 suggests for the exponent s in the scaling law (9) a value of 1.29. At the photospheric height the computations suggest a value of $s = 1.47$.

We should point out, however, that the convective velocities found in our models are large. As already indicated in Fig. 12, the turbulent Mach number $M_{\rm t}$ becomes relatively large for models with $M/M_\odot \gtrsim 1.4$. Relative to a local convection model, the nonlocal formulation used here reduces the convective velocities, although they still remain large. This reduction results in part from the averaging of the superadiabatic temperature gradient over the eddies, which spreads the influence of this gradient's sharp peak in the hydrogen ionization zone over a larger region.

8.4. Dependence on mixing length and metallicity

The dependence of the luminosity amplitudes on mixing-length parameter α and metallicity Z is illustrated in Fig. 16 over a

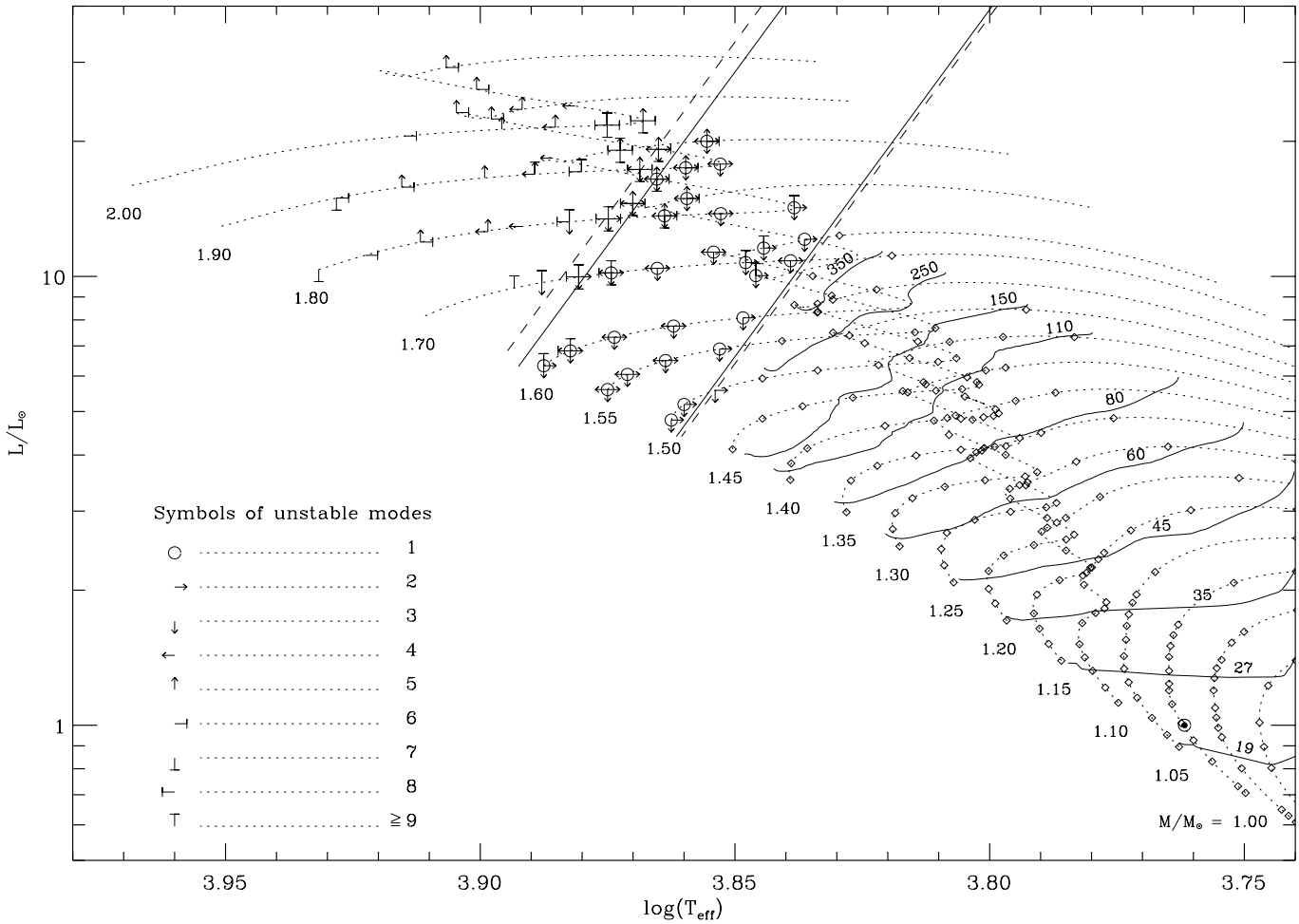

Fig. 13. Unstable modes and mean velocity amplitudes of stochastically excited oscillations. Amplitudes, evaluated at a height h=200 km are depicted as contours (solid curves) labelled at the amplitude values 19, 27, 35, 45, 60, 80, 110, 150, 250, 350 cm s^{-1}. The dotted curves are evolutionary tracks. The Sun, indicated by its symbol $\odot$, exhibits a mean (rms) velocity of 20.0 cm s^{-1}. Calculations have been carried out till the end of hydrogen core-burning, giving the low-temperature extremities of the contours. The location of the instability strips for the $n = 1$ and $n = 2$ radial modes are indicated by solid and dashed straight lines, respectively.

range of effective temperature for models with constant luminosity. The dependence of the velocity amplitudes are illustrated in Fig. 17 for two evolving models with mass $1.0M_\odot$ and $1.3M_\odot$.

Increasing the mixing-length parameter results in an increase of both the luminosity and velocity amplitudes (top panels). This comes about because increasing α results in higher convective velocities u and thus in a larger acoustic generation rate $P_{\rm Q}$ (see Eq. 8). Moreover, it appears that the amplitudes become less dependent upon α with increasing luminosity, which might be explained by the decrease in convective efficacy with model mass.

A similar behaviour of the amplitudes is obtained when the metallicity is increased (bottom panels in Figs 16 and 17). A larger value for the heavy-element abundance Z results in a higher opacity κ and consequently in a larger convective heat flux in the upper boundary layer of the convection zone. Therefore the turbulent Mach number $M_{\rm t}$ becomes larger, and thus also do the amplitudes.

9. Overstable modes

For stars with $\log T_{\rm eff} \gtrsim 3.85$ lying more or less in the δ Scuti instability strip, the model calculations predict modes to be overstable, irrespectively of adjustments to the convection parameters a and b. The δ Scuti stars are variables with spectral types A and F in the lower part of the classical Cepheid instability strip, which are in the very interesting evolutionary phase of the main sequence near the end of central hydrogen burning. It was first shown by Zhevakin (1953) and Cox & Whitney (1958) that the excitation mechanism in Cepheids, which are core-helium-burning radial pulsators having large amplitudes of the fundamental mode (and in a few cases also the first overtone), is plausibly due to the opacity mechanism acting in the HeII ionization zone (see also Baker & Kippenhahn 1962). The same mechanism is believed to be responsible for the excitation in δ Scuti stars (e.g. Dziembowski 1995 and references therein). The oscillation spectra of many δ Scuti stars, however, are far more complex, involving both radial and nonradial modes with

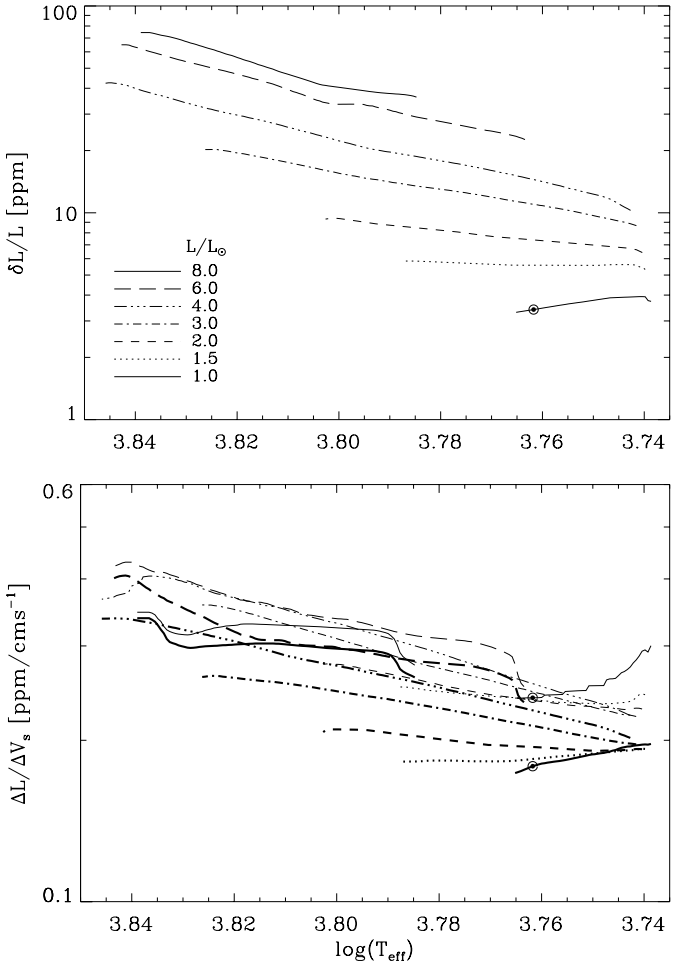

Fig. 14. Luminosity amplitudes (top) and amplitude ratios (bottom) as function of effective temperature and model luminosity. The amplitude ratios are displayed for velocities at two different atmospheric levels: the thin curves denote the results at $h = 0$ km and the thick curves at the height $h = 200$ km. The luminosity amplitudes are computed at the outermost meshpoint of the models. The computations assumed model parameters as given in Fig. 4. The value for the Sun (3.4 ppm) is indicated by its symbol.

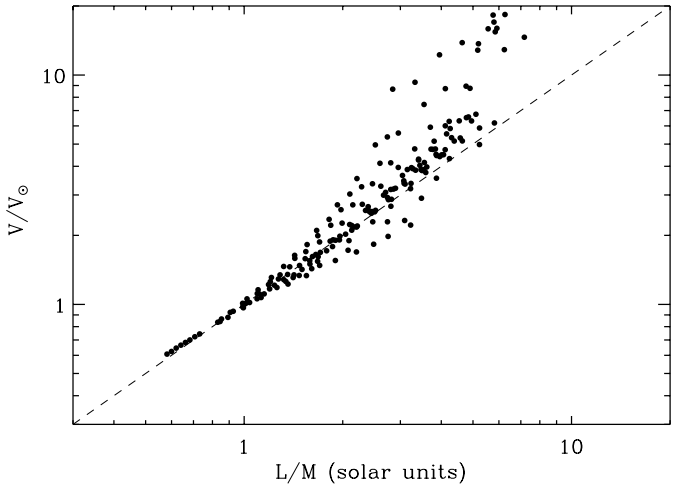

Fig. 15. Velocity amplitudes as function of light-to-mass ratio for stochastically excited oscillations in 191 models (filled circles) calculated at a height h=200 km above the photosphere with the same convection parameters as for Fig. 4. The dashed curve indicates Kjeldsen & Bedding's scaling law (9) with $s = 1$. The amplitudes are displayed relative to the value found in the Sun.

low amplitudes, lying often in a narrow frequency range. This complicates mode identification substantially (e.g. Mangeney et al. 1991). The cooler δ Scuti stars have substantial outer convection zones. Thus in these layers the pulsationally induced fluctuations of the turbulent fluxes may become important for the selection mechanism of modes with observable amplitudes.

The theoretically predicted order n of unstable p modes in sequences of evolving models of δ Scuti stars are depicted by different symbols in Fig. 13 (e.g. circles indicate the location of models in the HR diagram for which the radial fundamental mode was found to be overstable). The models have only a few excited modes lying in a narrow frequency interval, and some of them display radial orders in a nonconsecutive sequence (however, see also Houdek & Gough 1998; Michel et al. 1999). Moreover, with increasing effective temperature the overstable modes shift to higher frequencies. The blue edge of the instability domain is found to shift to higher effective temperatures with increasing order; this result is consistent with previous model calculations (e.g. Stellingwerf 1979, 1980; Dziembowski 1995) mainly because for these models convection is unimportant. Through the inclusion of the turbulent flux perturbations in the stability analyses the computations predict well defined red edges, a result which was previously reported by Baker & Gough (1979) for RR Lyrae stars. In particular, the fluctuating Reynolds stress $\delta p_{\rm t}$ is found to be the decisive contributor to the damping rates and thus for the return to stability at the red edge for low-order modes in δ Scuti stars (Houdek 1997). Only with the inclusion of $\delta p_{\rm t}$ in the computations are all modes found to be stable for models with effective temperatures satisfying $\log T_{\rm eff} \lesssim 3.85$.

10. Conclusion

It is evident that one of the greatest deficiencies in modelling oscillations in stars with surface convection zones is the lack of a proper theory of convection in a pulsating environment. Although several attempts have been made in recent years to address this problem (for a review, see Baker 1987) none of the proposed prescriptions are anything more than phenomenological. Impressive progress has been made on hydrodynamical simulations of convection, including also the interaction with pulsations (e.g. Stein & Nordlund 1991; Bogdan et al. 1993; Nordlund & Stein 1998; Stein & Nordlund 1998). In particular, the work by Stein and Nordlund, including a realistic treatment of the physics of the outer parts of the convection zone, has confirmed the earlier conclusion that the solar oscillations are likely to be intrinsically stable (e.g. Gough 1980; Kumar & Goldreich 1989; Balmforth 1992a); also, the simulations yielded estimates, similar to the observationally determined values, of

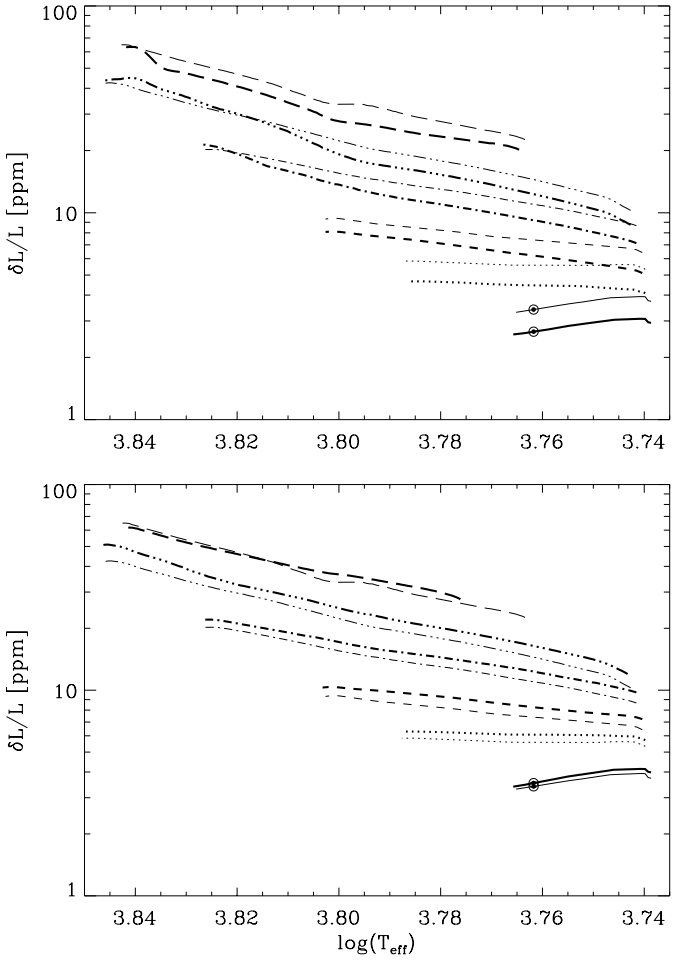

Fig. 16. Luminosity amplitudes (computed at outermost meshpoint) versus effective temperature for models with constant luminosity. The results are displayed for different mixing-length parameters α (top) and metallicities (bottom). The computations assumed the nonlocal convection parameters of Fig 4. The line styles are as defined in Fig. 14. *Top:* the thick curves display the results for models computed with $\alpha = 1.8$ and the thin curves depict the amplitudes obtained with $\alpha = 2.0$. In both model sequences the value for the metallicity Z was chosen to be 0.02. *Bottom:* the thick curves depict the amplitudes from model calculations using $Z = 0.04$ and the thin curves for $Z = 0.02$, assuming $\alpha = 2.0$.

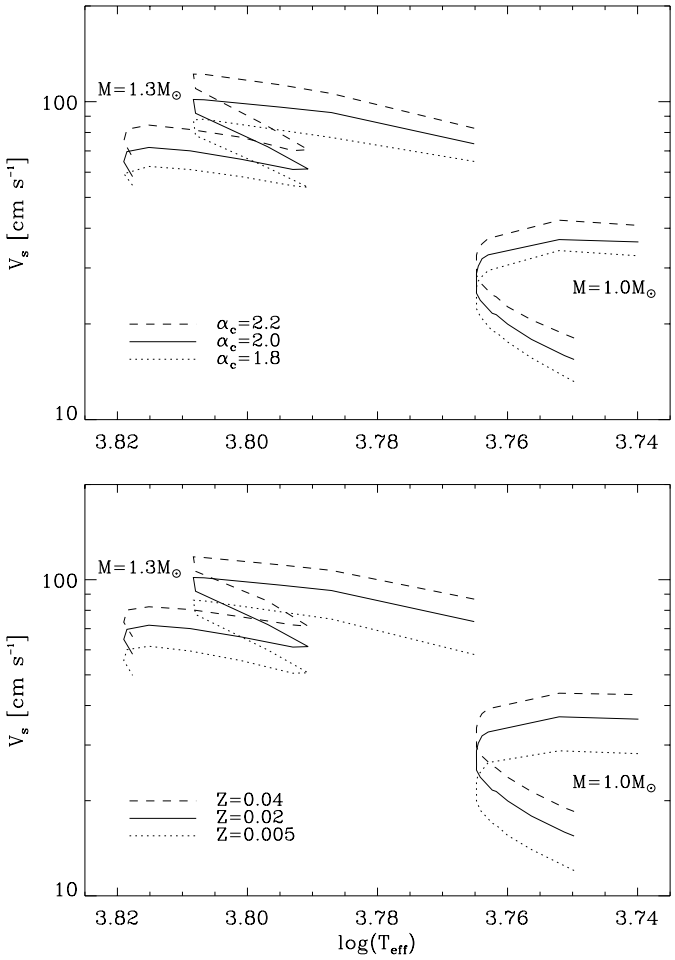

Fig. 17. Velocity amplitudes for an evolving $1.0M_\odot$ and $1.3M_\odot$ star versus the model's effective temperature. The computations assumed the nonlocal convection parameters of Fig. 4 and results are displayed at a photospheric level $h = 200$ km. *Top:* amplitudes are depicted for three values of of the mixing-length parameter α assuming $Z = 0.02$ in the computations. *Bottom:* results are plotted for three values of metallicity Z assuming $\alpha = 2.0$ in the model calculations.

the energy input to the modes from the stochastic driving by convection. However, such simulations are evidently extremely time consuming and have so far been made in sufficient detail only for solar parameters. Here we have estimated the pulsational properties of main-sequence stars over a broad range of parameters, by means of a time-dependent non-local version of mixing-length theory.

Perhaps the most important conclusion drawn from this survey is that, as in the case of the Sun, oscillations in solar-like stars are intrinsically damped and stochastically driven by convection. We note that the issue may still not be entirely settled, however. In particular, Cheng & Xiong (1997) reported calculations using Xiong's (1989) nonlocal formulation of mixing-length theory which predict overstable solar oscillations. In fact, their computations suggest that the momentum flux perturbations destabilize all p modes, in complete disagreement to the results reported here. This discrepancy evidently deserves investigation.

Acknowledgements. We are grateful to W. Chaplin for providing us with the latest BiSON data. This work was supported in part by Danmarks Grundforskningsfond through the establishment of the Theoretical Astrophysics Center and by the Particle Physics and Astronomy Research Council of the UK. G.H. acknowledges travel support by the Austrian FWF (project S7303-AST).

References

Antia H.M., Chitre S.M., Gough D.O., 1988, in: Proc. IAU Symposium No 123, Advances in helio- and asteroseismology, Christensen-Dalsgaard J., Frandsen S. (eds). Reidel, Dordrecht, p. 371

Appourchaux T. and the VIRGO team, 1998, in: Structure and dynamics of the interior of the Sun and Sun-like stars; Proc. SOHO

6/GONG 98 Workshop, Korzennik, S.G., Wilson, A. (eds). ESA SP-418, Noordwijk, p. 99
Auer L.H., Mihalas D., 1970, MNRAS 149, 65
Baker N.H., 1987, in: Physical Processes in Comets, Stars and Active Galaxies, Hillebrandt, W., Meyer-Hofmeister, E., Thomas, H.-C. (eds). Springer-Verlag, New York, p. 105
Baker N.H., Kippenhahn R., 1962, Zs. f. Ap. 54, 114
Baker N.H., Kippenhahn R., 1965, ApJ 142, 868
Baker N.H., Gough D.O., 1979 ApJ, 234,232
Baker N.H., Moore D.W., Spiegel E.A., 1971, Q. J. Mech. Appl. Math. 24, 391
Balmforth N.J., 1992a, MNRAS 255, 603
Balmforth N.J., 1992b, MNRAS 255, 639
Balmforth N.J., Gough D.O., 1990a, SPh 128, 161
Balmforth N.J., Gough D.O., 1990b, ApJ 362, 256
Batchelor G.K., 1956, The theory of homogeneous turbulence, Cambridge University Press
Bedding T.R., Kjeldsen H., Reetz J, Barbuy B., 1996, MNRAS 280, 1155
Bogdan T.J., Cattaneo F., Malagoli A., 1993, ApJ 407, 316
Böhm-Vitense E., 1958, Zs. F. Ap. 46, 108
Brown T.M., Gilliland R.L., 1990, ApJ 350, 839
Brown T.M., Gilliland R.L., Noyes R.W., Ramsey L.W., 1991, ApJ 368, 599
Canuto V.M., Christensen-Dalsgaard J., 1998, Ann. Rev. Fluid Mech. 30, 167
Catala C. and the COROT team, 1995, in: Proc. GONG'94 Helio- and Astero-seismology from Earth and Space, Ulrich, R.K., Rhodes Jr, E.J., Däppen, W. (eds). PASPC 76, San Francisco, p. 426
Chang H-Y., Gough D.O., Sekii T., 1997, in: Proc. IAU Symp. 181: Sounding Solar and Stellar Interiors, Schmider, F.-X., Provost, J. (eds). Nice Observatory, Poster Volume, p. 13
Chaplin W.J., Elsworth Y., Isaak G.R., Lines R., McLeod C.P., Miller B.A., New R., 1998, MNRAS 298, 7
Cheng Q.L., Xiong D.R., 1997, A&A 319, 981
Christensen-Dalsgaard J., 1982, MNRAS 199, 735
Christensen-Dalsgaard J., 1993, in: Inside the Stars, Weiss, W.W., Baglin, A. (eds). PASPC 40, San Francisco, p. 483
Christensen-Dalsgaard J., Frandsen S., 1983a, SPh 82, 165
Christensen-Dalsgaard J., Frandsen S., 1983b, SPh 82, 469
Christensen-Dalsgaard J., Gough D.O., 1982, MNRAS 198, 141
Christensen-Dalsgaard J., Gough D.O., Libbrecht K.G., 1989, ApJ 341, L103
Cox J.P., Whitney C., 1958, ApJ 127, 561
Dziembowski W.A., 1995, in: Proc. GONG'94: Helio- and Astero-seismology from Earth and Space, Ulrich, R.K., Rhodes Jr, E.J., Däppen, W. (eds). PASPC 76, San Francisco, p. 586
Elsworth Y., Howe R., Isaak G.R., Mcleod C.P., Miller B.A., New R., Speake, C.C., Wheeler S.J., 1993, MNRAS 265, 888
Eggleton P., Faulkner J., Flannery B.P., 1973, A&A 23, 325
Frandsen S., 1992, in: Inside the Stars, Weiss W.W., Baglin A. (eds). PASPC 40, San Francisco, p. 679
Fröhlich C. and the VIRGO team, 1995, SPh 162, 101
Gabriel M., 1998, A&A 330, 359
Gabriel A.H. and the GOLF team, 1991, Adv. Space Res., vol. 11, No. 4, 103
Gilliland R.L., 1995, in: Proc. GONG'94: Helio- and Astero-seismology from Earth and Space, Ulrich, R.K., Rhodes Jr, E.J., Däppen, W. (eds). PASPC 76, San Francisco, p. 578
Gilliland R.L., Brown T.M., Kjeldsen H., McCarthy J.K., Peri M.L., Belmonte J.A., Vidal I., Cram L.E., Palmer J., Frandsen S., Parthasarathy M., Petro L., Schneider H., Stetson P.B., Weiss W.W., 1993, AJ 106, 2441
Goldreich P., Keeley D.A., 1977a, ApJ 211, 934
Goldreich P., Keeley D.A., 1977b, ApJ 212, 243
Goldreich P., Kumar P., 1990, ApJ 363, 694
Goldreich P., Kumar P., 1991, ApJ 374, 366
Goldreich P., Murray N., 1994, ApJ 424, 480
Goldreich P., Murray N., Kumar P., 1994, ApJ 423, 466
Gonczi G., Osaki Y., 1980, A&A 84, 304
Goode P.R., Strous L.H., 1996, Bull. Astr. Soc. India 24, 223
Goode P.R., Gough D.O., Kosovichev A., 1992, ApJ 387, 707
Gough D.O., 1965, in: Geophysical Fluid Dynamics II, Woods Hole Oceanographic Institution, p. 49
Gough D.O., 1976, in: Problems of stellar convection, Spiegel, E., Zahn, J.-P. (eds). Springer-Verlag, Berlin, p. 15
Gough D.O., 1977, ApJ 214, 196
Gough D.O., 1980, in: Nonradial and Nonlinear Stellar Pulsation, Hill, H.A., Dziembowski, W.A. (eds). Springer-Verlag, Berlin, p. 273
Gough D.O., 1995, in: Proc. GONG'94: Helio- and Astero-seismology from Earth and Space, Ulrich, R.K., Rhodes Jr, E.J., Däppen, W. (eds). PASPC 76, San Francisco, p. 331
Gough D.O., 1997, in: Proc. IAU Symp. 181: Sounding Solar and Stellar Interiors, Schmider, F.-X., Provost, J. (eds). Nice Observatory, p. 397
Gough D.O., Weiss N.O., 1976, MNRAS 176, 589
Gough D.O., Spiegel E.A., Toomre J., 1974, Lecture Notes in Physics 35, Richtmeyer, R. (ed.). Springer-Verlag, Heidelberg
Grec G., Fossat E., Pomerantz M., 1983, SPh 82, 55
Harvey J.W., Hill F., Hubbard R.P., et al., 1996, Science 272, 1284
Henyey L., Vardya M.S., Bodenheimer P., 1965, ApJ 142, 841
Hill F., Stark P.B., Stebbins R.T., et al., 1996, Science 272, 1292
Houdek G., 1996, Ph.D. Thesis, Universität Wien
Houdek G., 1997, in: Proc. IAU Symp. 181: Sounding Solar and Stellar Interiors, Schmider, F.-X., Provost, J. (eds). Nice Observatory, Poster Volume, p. 227
Houdek G., Rogl J., 1996, Bull. Astr. Soc. India 24, 317
Houdek G., Gough D.O., 1998, in: Structure and dynamics of the interior of the Sun and Sun-like stars; Proc. SOHO 6/GONG 98 Workshop, Korzennik, S.G., Wilson, A. (eds). ESA SP-418, Noordwijk, p. 479
Houdek G., Rogl J., Balmforth N., Christensen-Dalsgaard J., 1995, in: Proc. GONG'94: Helio- and Astero-seismology from Earth and Space, Ulrich, R.K., Rhodes Jr, E.J., Däppen, W. (eds). PASPC 76, San Francisco, p. 641
Iglesias C.A., Rogers F.J., 1996, ApJ 464, 943
Kennelly E.J., 1995, in: Proc. GONG'94: Helio- and Astero-seismology from Earth and Space, Ulrich, R.K., Rhodes Jr, E.J., Däppen, W. (eds). PASPC 76, San Francisco, p. 568
Jefferies S.M., Pallé P.L., van der Raay H.B., Régulo C., Roca Cortés T., 1988, Nature 333, 646
Kjeldsen H., Bedding T.R., 1995, A&A 293, 87
Kjeldsen H., Bedding T.R., 1998, in: Proc. First MONS Workshop, Kjeldsen, H., Bedding, T.R. (eds). Aarhus Universitet, Denmark, p. 1
Kjeldsen H., Bedding T.R., Viskum M., Frandsen S., 1995, AJ 109, 1313
Kumar P., Goldreich P., 1989, ApJ 103, 331
Kurucz R.L., 1991, in: Stellar Atmospheres: Beyond Classical Models, Crivellari, L., Hubeny, I., Hummer, D.G. (eds). Kluwer, Dordrecht, p. 441
Lamb H., 1909, Proc. London Math. Soc. 7, 122
Libbrecht K.G., 1988, ApJ, 334, 510
Libbrecht K.G., Woodard M.F., 1991, Science 253, 152

Libbrecht K.G., Popp B.D., Kaufman J.M., Penn M.J., 1986, Nature 323, 235
Mangeney A., Däppen W., Praderie F., Belmonte J.A., 1991, A&A 244, 351
Matthews J.M., 1998, in: Structure and dynamics of the interior of the Sun and Sun-like stars; Proc. SOHO 6/GONG 98 Workshop, Korzennik, S.G., Wilson, A. (eds). ESA SP-418, Noordwijk, p. 395
Michel E., Hernández M.M., Houdek G., Goupil M.J., Lebreton Y., Hernández F.Pérez, Baglin A., Belmonte J.A., Soufi F., 1999, A&A 342, 153
Moore, D.W., Spiegel E.A., 1964, ApJ 139, 48
Mosser B., Maillard J.P., Mékarnia D., Gay J., 1998, A&A 340, 457
Musielak Z.E., Rosner R., Stein R.F., Ulmschneider P., 1994, ApJ 423, 474
Nigam R., Kosovichev A.G., Scherrer P.H., Schou J., 1998, ApJ 495L, 115N
Nordlund Å., Stein R.F., 1998, in: Proc. IAU Symp. 185: New eyes to see inside the Sun and stars, Deubner, F.-L., Christensen-Dalsgaard, J., Kurtz, D.W. (eds). Kluwer, Dordrecht, p. 199
Osaki Y., 1990, in: Progress of Seismology of the Sun and Stars, Osaki, Y., Shibahashi, H. (eds). Springer-Verlag, Berlin, p. 145
Rast M.P., Bogdan T.J., 1998, ApJ 496, 527
Rosenthal C.S., Christensen-Dalsgaard J., Houdek G., Monteiro M.J.P.F.G., Nordlund Å., Trampedach R., 1995, in: Proc. 4th SOHO Workshop: Helioseismology, Hoeksema, J.T., Domingo, V., Fleck, B., Battrick, B. (eds). ESA SP-376, vol.2, ESTEC, Noordwijk, p. 459
Roxburgh I.W., Vorontsov S.V., 1997, MNRAS 292, L33
Scherrer P.H., Hoeksema J.T., Bush R.I., 1991, Adv. Space Res., vol. 11, No. 4, 113
Schrijver C.J., Jiménez A., Däppen W., 1991, A&A 251, 655
Spiegel E., 1962, J. Geophys. Res. 67, 3063
Spiegel E., 1963, ApJ 138, 216
Stein R.F., 1967, SPh 2, 385
Stein R.F., Nordlund Å., 1991, in: Challenges to Theories of the Structure of Moderate Mass Stars, Gough, D.O., Toomre, J. (eds). Springer-Verlag, Heidelberg, p. 195
Stein R.F., Nordlund Å., 1998, in: Structure and dynamics of the interior of the Sun and Sun-like stars; Proc. SOHO 6/GONG 98 Workshop, Korzennik S.G., Wilson A. (eds). ESA SP-418, Noordwijk, p. 693
Stellingwerf R.F., 1979, ApJ 227, 935
Stellingwerf R.F., 1980, in: Nonradial and Nonlinear Stellar Pulsation, Hill, H.A., Dziembowski, W.A. (eds). Springer-Verlag, Berlin, p. 50
Tooth P.D., Gough D.O., 1989, in: Seismology of the Sun and Sun-like Stars, Domingo, V., Rolfe, E. (eds). ESA SP-286, Noordwijk, p. 463
Toutain T., Fröhlich C., 1992, A&A 257, 287
Ulrich R.K., 1970a, ApJ 162, 993
Ulrich R.K., 1970b, Ap&SS 7, 71
Unno W., 1964, Trans. Int. astr. Un. XII(B), 555
Unno W., 1967, PASJ 19, 140
Unno W., Kato S., 1962, PASJ 14, 416
Unno W., Spiegel E.A., 1966, PASJ 18, 85
Vernazza J.E., Avrett E.H., Loeser R., 1981, ApJS 45, 635
Xiong D., 1989, A&A 254, 362
Zhevakin S.A., 1953, Astron. Zh. 30, 161